

Global Conformational Dynamics in Ras[†]

Casey O'Connor and Evgenii L. Kovrigin*

Department of Biochemistry, Medical College of Wisconsin, 8701 Watertown Plank Road, Milwaukee, Wisconsin 53226

Received June 6, 2008; Revised Manuscript Received August 15, 2008

ABSTRACT: Ras and its homologues are central to regulation of a multitude of cellular processes. Ras in complex with GTP binds and activates its downstream signaling partners. ³¹P NMR studies indicated that the Ras–GTP conformation is heterogeneous on a millisecond time scale, but details of its conformational dynamics remain unknown. Here we present evidence that the conformational exchange process in human H-Ras complexed with GTP mimic GppNHp is global, encompassing most of the GTPase catalytic domain. The correlated character of conformational dynamics in Ras opens opportunities for understanding allosteric effects in Ras function.

Ras GTPase and its homologues act as molecular switches in a variety of intracellular processes, including signal transduction, growth, proliferation, and apoptosis (see reviews in refs 1–4). The conventional view of their mechanism of action implies interconversion between two distinct conformational states: an effector-competent state complexed with GTP and an inactive GDP-bound conformation with a low affinity for effectors (4). Recent ³¹P NMR studies suggested that active, GTP-loaded Ras is a mix of two distinct conformers in dynamic equilibrium, one being an effector-competent conformation (“state 2”) and the nature of the other (“state 1”) remaining unknown (5–9). Phosphorus NMR studies by Liao and co-workers demonstrated that this observed conformational heterogeneity is common for a number of Ras homologues (10).

All previous studies revealing two distinct conformations in Ras loaded with uncleavable GTP mimic were performed by monitoring the splitting of NMR signals from the phosphorus atoms of the nucleotide phosphate backbone. Very little is reported concerning conformational rearrangement in Ras tertiary structure involved in the dynamics of the phosphorus nuclei. One of the likely causes of this dynamics was proposed to be as simple as a single Y32 side chain flipping out from the active site (5). However, mutational analysis indicated that these dynamic rearrangements are not simply localized to the immediate vicinity of Y32 (7).

Heteronuclear NMR spectroscopy is the most powerful technique for detailing conformational dynamics of proteins in solution. Spin-relaxation NMR experiments are capable of detecting conformational dynamics with site-specific resolution (for reviews, see refs 11–13). A study by Ito and

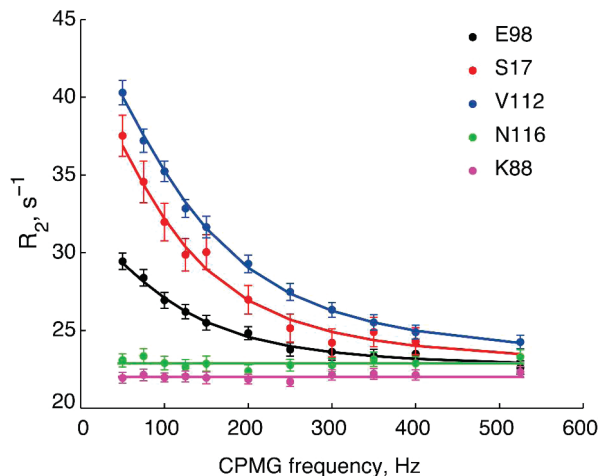


FIGURE 1: Transverse relaxation rate constants for 1 mM H-Ras-(1–166)•GppNHp obtained in ¹⁵N rcCPMG spin relaxation NMR experiments at 14.1 T, 17 °C, and pH 7.4. Curves correspond to fitting results by the all-timescale two-state exchange model.

co-workers revealed extreme broadening of resonances in switch regions of H-Ras complexed with different GTP mimics (14). ³¹P NMR data indicated that the conformational exchange occurs on a millisecond time scale (6). Faster, subnanosecond dynamics have been examined for the GDP-bound state of H-Ras (15, 16), but millisecond time scale dynamics for either GDP- or GTP-bound forms have never been addressed. To elucidate details of the millisecond conformational rearrangements in the active form of Ras, we performed ¹⁵N spin relaxation rcCPMG measurements (17, 18) with the GTPase catalytic domain (residues 1–166) of human H-Ras complexed with the slowly hydrolyzable GTP mimic, GppNHp. Experiments were carried out at a static magnetic field strength of 11.7 T at four temperatures (7, 12, 17, and 22 °C) and at 14.1 T and 17 °C. Experimental details are given in the Supporting Information.

Figure 1 shows profiles of the amide ¹⁵N transverse relaxation rate as a function of CPMG pulse train frequency for representative residues in the H-Ras•GppNHp complex. When measuring the relaxation rate in a rcCPMG experiment, we observe the effect of conformational exchange on the transverse relaxation rate constant, R_2 . Conformational exchange causes an increase in the apparent R_2 ; increasing the CPMG frequency in the experiment weakens this effect. Therefore, nuclei experiencing significant conformational or chemical exchange demonstrate dispersions of R_2 values determined over a range of CPMG frequencies (examples in Figure 1, V112, E98, and S17). Residues with little or no contribution from microsecond to millisecond dynamics to ¹⁵N relaxation exhibit flat featureless profiles (exemplified here by K88 and N116).

[†] This work was supported by Grant IRG-86-004 from the American Cancer Society and by the Cancer Center of the Medical College of Wisconsin.

* To whom correspondence should be addressed. Phone: (414) 955-5885. Fax: (414) 456-6510. E-mail: ekovrig@mcw.edu.

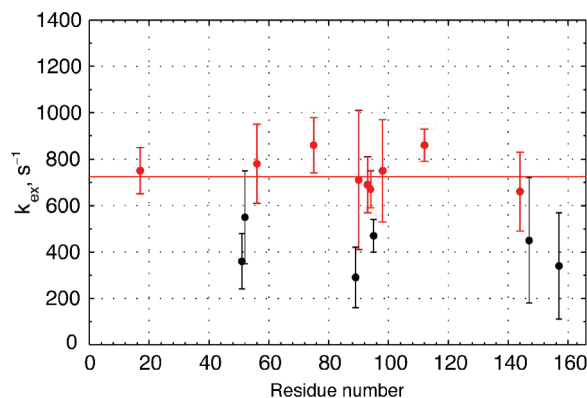


FIGURE 2: Exchange rate constants at 17 °C determined from simultaneous fitting of data obtained at static magnetic fields of 11.7 T (at 7, 12, 17, and 22 °C) and 14.1 T (at 17 °C). Red symbols denote a group of residues successfully fit to a global exchange model with a common $k_{\text{ex}}(17\text{ °C})$ of 720 ± 30 (shown by a red line).

The H-Ras GTPase catalytic domain has a total of 166 residues. We were able to perform relaxation measurements for 75 sufficiently resolved and high-intensity peaks. A significant conformational exchange contribution to relaxation was observed for amide nitrogen resonances of 20 residues: L6, S17, T20, N26, C51, L56, G75, N85, S89, F90, I93, H94, Q95, Y96, E98, V112, T144, K147, and Y157. We fit every residue using data obtained at two static magnetic fields of 11.7 T (at 7, 12, 17, and 22 °C) and 14.1 T (at 17 °C) with the general all-timescale equation for the two-site conformational exchange (19) using CPMG_FITD8 (20). Details of the fitting procedure are given in the Supporting Information. Exchange rate constant k_{ex} determined for 15 residues with sufficient data quality is shown in Figure 2. A group of nine residues [S17, L56, G75, F90, I93, H94, E98, V112, and T144 (red symbols)] forms a cluster with similar k_{ex} values, suggesting that they may respond to the same exchange process. Global fitting of this group of nine residues using the data from both static magnetic fields at 17 °C and from the field of 11.7 T at 7, 12, and 22 °C yields a k_{ex} value at 17 °C of $720 \pm 30\text{ s}^{-1}$. The activation enthalpy determined from the temperature dependence of k_{ex} is $50 \pm 8\text{ kJ/mol}$. The group of residues occurs in the fast exchange regime (with the largest ^{15}N chemical shift difference between the two conformers of $\sim 400\text{ s}^{-1}$ at the V112 amide group), thus making fitted values of conformer populations unreliable (21). To improve the definition of populations of the exchanging states, one needs multifield data at lower temperatures where the exchange regime shifts to intermediate, and this work is currently underway.

The spatial distribution of dynamic residues in the tertiary structure of Ras is shown in Figure 3. It is remarkable that dynamic residues are both found adjacent to the exchange-broadened switch regions and nucleotide-binding site (S17, T20, N26, L56, and K147) as well as throughout the entire GTPase catalytic domain, i.e., G75 (18.9 Å from the γ -phosphorus atom of GppNHp), E98 (19.1 Å), and V112 (18.5 Å). The similarity of the exchange rate constants at these sites as well as significant spatial separation of these residues from the effector interface and from each other (i.e., 13.2 Å from G75 to V112, 14.6 Å from G75 to E98, and 23.1 Å from G75 to T144) strongly suggests that a cause of

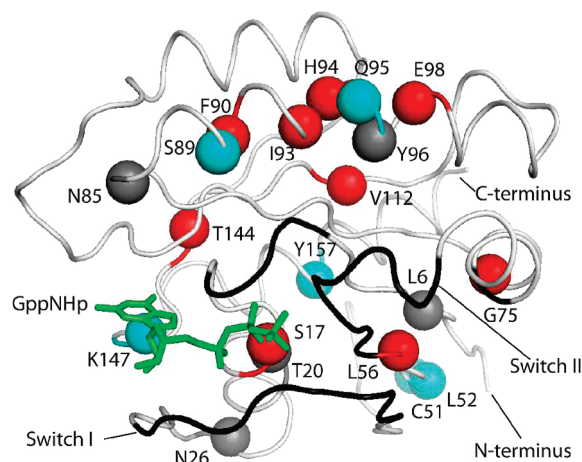


FIGURE 3: Molecular model of the GTPase catalytic domain of residues 1–166 of human H-Ras complexed with GTP mimic GppNHp [PDB entry 5P21 (22)]. The protein backbone is shown as a tube. GppNHp is displayed in a green stick representation. The protein is oriented with its GTPase binding site and effector interaction interface facing the reader. Black tube coloring indicates the residues of the switch regions and the P-loop, undetectable in HSQC spectra of the Ras•GppNHp complex due to extreme exchange broadening (14). Spheres depict the amide nitrogen atoms of resolved residues with measurable relaxation dispersions. Red denotes residues with similar k_{ex} values (corresponding to red symbols in Figure 2). Cyan shows other quantifiable dynamic residues (black symbols in Figure 2). Gray spheres denote dynamic residues for which the signal:noise ratio was insufficient for accurate determination of the exchange rate.

exchange contributions to ^{15}N relaxation at these sites must be an extensive conformational rearrangement (“breathing”) of the major part of Ras structure on a millisecond time scale.

Conformational dynamics at switch regions and the P-loop broadens signals from a number of residues beyond detection (Figure 3 and Figure S2 of the Supporting Information) (14). We may speculate that the dynamics observed in our study is related to the exchange process at the nucleotide binding site and effector interface because some of the dynamic residues are members of the conserved G-boxes (Figure S2): S17 belongs to G1 (P-loop), L56 belongs to G3, T144 and K147 belong to G5, and others (T20 and N26) are close to the P-loop and switch I. A more distant location of residues from the effector interface (switches I and II) may lead to smaller motional amplitudes (with a corresponding reduced effect on chemical shifts), thus rendering these amide nitrogens detectable yet reporting on the same exchange process.

The role the global conformational exchange plays in the biological function of Ras remains unclear. It is unlikely that nucleotide association and dissociation cause this dynamics because, by our estimate, k_{ex} due to GppNHp binding is at least 2 orders of magnitude lower than the exchange rate of global conformational dynamics at the same temperature (see the Supporting Information for details). Transient kinetic studies of the interaction of Ras with the immediate downstream effector c-Raf-1 (using its Ras-binding domain, residues 51–131) by stopped-flow fluorescence measurements revealed a two-step binding reaction mechanism with formation of the weak first-encounter complex followed by an isomerization step leading to the tight-binding conformation (23). The rate of the isomerization step was estimated to be on the order of 780 s^{-1} at 10 °C and 1380 s^{-1} at 15

°C, which corresponds to activation enthalpy of ~ 77 kJ/mol. This value is similar to the activation enthalpy of transition between states 1 and 2 observed by ^{31}P NMR in GppNHp-loaded H-Ras 1–166 (~ 70 kJ/mol), though measured rates were lower ($k_{12} = 250 \text{ s}^{-1}$ and $k_{21} = 135 \text{ s}^{-1}$ at 15°C) (6, 8, 9). Extrapolation of k_{ex} at 15°C from our data produces an estimate of $650 \pm 30 \text{ s}^{-1}$ and activation enthalpy of 50 ± 8 kJ/mol for the global conformational exchange process in Ras tertiary structure. Comparing these values to the exchange rate for state 1–state 2 equilibrium $k_{\text{ex}} = k_{12} + k_{21} = 385 \text{ s}^{-1}$ (8) as well as to the rate of the isomerization step in the interaction of Ras with Raf-RBD and their corresponding activation enthalpies, we may hypothesize that all three observations may be related to one conformational exchange process with the observed differences being caused by differing solution conditions. Direct kinetic measurements of the interaction of Ras with nucleotide and effectors coupled with spin relaxation and NMR line shape analysis of ^{31}P , ^{15}N , and ^{13}C nuclei in Ras structure could verify this hypothesis, and this work is currently in progress.

In summary, our ^{15}N spin relaxation data reveal that the structure of the Ras GTPase catalytic domain is not simply a rigid scaffold to which the nucleotide binding pocket and flexible effector recognition motifs are attached. Our results indicate that the major part of the Ras GTPase catalytic domain is involved in conformational exchange. The global conformational dynamic process may be a major contributor to the documented dynamics of the effector interaction interface as well as the slow isomerization step in Ras–effector interactions. The global conformational exchange process in Ras structure could potentially explain the effect of distant mutations on the biological function of Ras-like GTPases (24) via mutation-induced population shifts leading to altered affinities for binding partners of Ras. Global conformational motion could also provide natural means of communication between the nucleotide binding site and a newly defined switch region on the opposite face of the GTPase catalytic domain controlling the orientation of Ras at the membrane and signal output (25).

ACKNOWLEDGMENT

We thank Dr. Brian Volkman for critical reading of the manuscript.

SUPPORTING INFORMATION AVAILABLE

Details of sample preparation, NMR experiments, and data analysis. This material is available free of charge via the Internet at <http://pubs.acs.org>.

REFERENCES

1. Barbacid, M. (1987) *Annu. Rev. Biochem.* 56, 779–827.
2. Herrmann, C. (2003) *Curr. Opin. Struct. Biol.* 13, 122–129.
3. Takai, Y., Sasaki, T., and Matozaki, T. (2001) *Physiol. Rev.* 81, 153–208.
4. Vetter, I. R., and Wittinghofer, A. (2001) *Science* 294, 1299–1304.
5. Geyer, M., Schweins, T., Herrmann, C., Prisner, T., Wittinghofer, A., and Kalbitzer, H. R. (1996) *Biochemistry* 35, 10308–10320.
6. Spoerner, M., Herrmann, C., Vetter, I. R., Kalbitzer, H. R., and Wittinghofer, A. (2001) *Proc. Natl. Acad. Sci. U.S.A.* 98, 4944–4949.
7. Spoerner, M., Wittinghofer, A., and Kalbitzer, H. R. (2004) *FEBS Lett.* 578, 305–310.
8. Spoerner, M., Nuehs, A., Ganser, P., Herrmann, C., Wittinghofer, A., and Kalbitzer, H. R. (2005) *Biochemistry* 44, 2225–2236.
9. Spoerner, M., Nuehs, A., Herrmann, C., Steiner, G., and Kalbitzer, H. R. (2007) *FEBS J.* 274, 1419–1433.
10. Liao, J. L., Shima, F., Araki, M., Ye, M., Muraoka, S., Sugimoto, T., Kawamura, M., Yamamoto, N., Tamura, A., and Kataoka, T. (2008) *Biochem. Biophys. Res. Commun.* 369, 327–332.
11. Palmer, A. G. (2004) *Chem. Rev.* 104, 3623–3640.
12. Mittermaier, A., and Kay, L. E. (2006) *Science* 312, 224–228.
13. Kay, L. E. (2005) *J. Magn. Reson.* 173, 193–207.
14. Ito, Y., Yamasaki, K., Iwahara, J., Terada, T., Kamiya, A., Shirouzu, M., Muto, Y., Kawai, G., Yokoyama, S., Laue, E. D., Walchli, M., Shibata, T., Nishimura, S., and Miyazawa, T. (1997) *Biochemistry* 36, 9109–9119.
15. Kraulis, P. J., Domaille, P. J., Campbell-Burk, S. L., Van Aken, T., and Laue, E. D. (1994) *Biochemistry* 33, 3515–3531.
16. Thapar, R., Williams, J. G., and Campbell, S. L. (2004) *J. Mol. Biol.* 343, 1391–1408.
17. Loria, J. P., Rance, M., and Palmer, A. G. (1999) *J. Am. Chem. Soc.* 121, 2331–2332.
18. Tollinger, M., Skrynnikov, N. R., Mulder, F. A. A., Forman-Kay, J. D., and Kay, L. E. (2001) *J. Am. Chem. Soc.* 123, 11341–11352.
19. Carver, J. P., and Richards, R. E. (1972) *J. Magn. Reson.* 6, 89–105.
20. Korzhnev, D. M., Salvatella, X., Vendruscolo, M., Di Nardo, A. A., Davidson, A. R., Dobson, C. M., and Kay, L. E. (2004) *Nature* 430, 586–590.
21. Palmer, A. G., Kroenke, C. D., and Loria, J. P. (2001) *Methods Enzymol.* 338–339, 204–238.
22. Pai, E., Krengel, U., Petsko, G., Goody, R., Kabsch, W., and Wittinghofer, A. (1990) *EMBO J.* 9, 2351–2359.
23. Sydor, J. R., Engelhard, M., Wittinghofer, A., Goody, R. S., and Herrmann, C. (1998) *Biochemistry* 37, 14292–14299.
24. Heo, W. D., and Meyer, T. (2003) *Cell* 113, 315–328.
25. Abankwa, D., Hanzal-Bayer, M., Ariotti, N., Plowman, S. J., Gorfe, A. A., Parton, R. G., McCammon, J. A., and Hancock, J. F. (2008) *EMBO J.* 27, 727–735.

BI801076C